Supplementary Information

Electrochemical semi-sacrificial growth of self-supporting MOF-based electrode for urea electrooxidation-coupled water electrolysis

Jiang Ji[a,b], Yinsheng Wang[a,b], Changsheng Cao[b,*], Xin-Tao Wu[b], and Qi-Long Zhu[b,*]

[a]*College of Chemistry, Fuzhou University, Fuzhou 350002, China*

[b]*State Key Laboratory of Structural Chemistry and Fujian Provincial Key Laboratory of Materials and Techniques toward Hydrogen Energy, Fujian Institute of Research on the Structure of Matter, Chinese Academy of Sciences, Fuzhou 350002, China*

**Corresponding author.*

E-mail addresses: cscao@fjirsm.ac.cn (C. Cao), and qlzhu@fjirsm.ac.cn (Q.-L. Zhu).

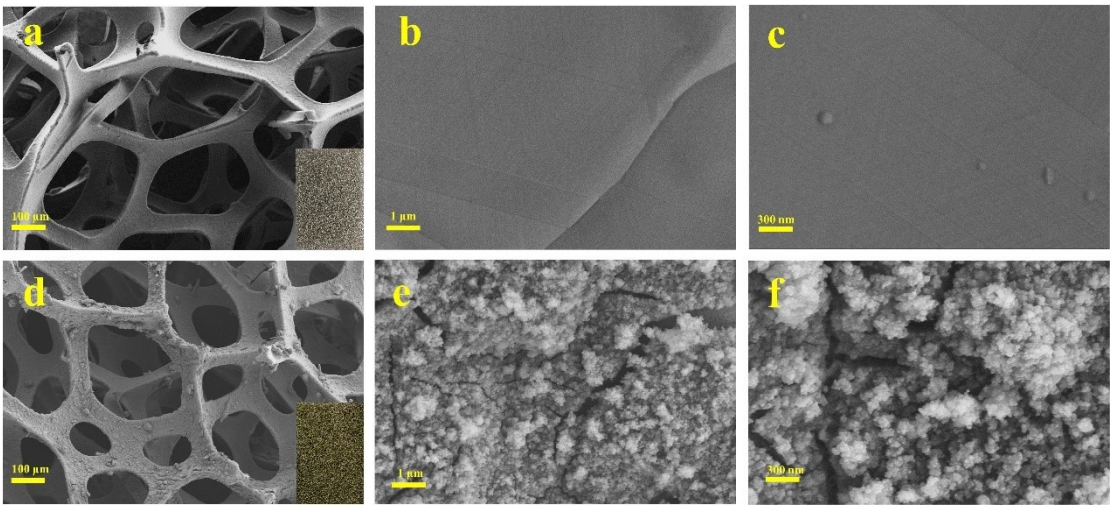

Fig. S1 SEM images of (a-c) NF and (d-f) NiFe-PBA-NF. Insets in (a) and (d) are the corresponding optical photos.

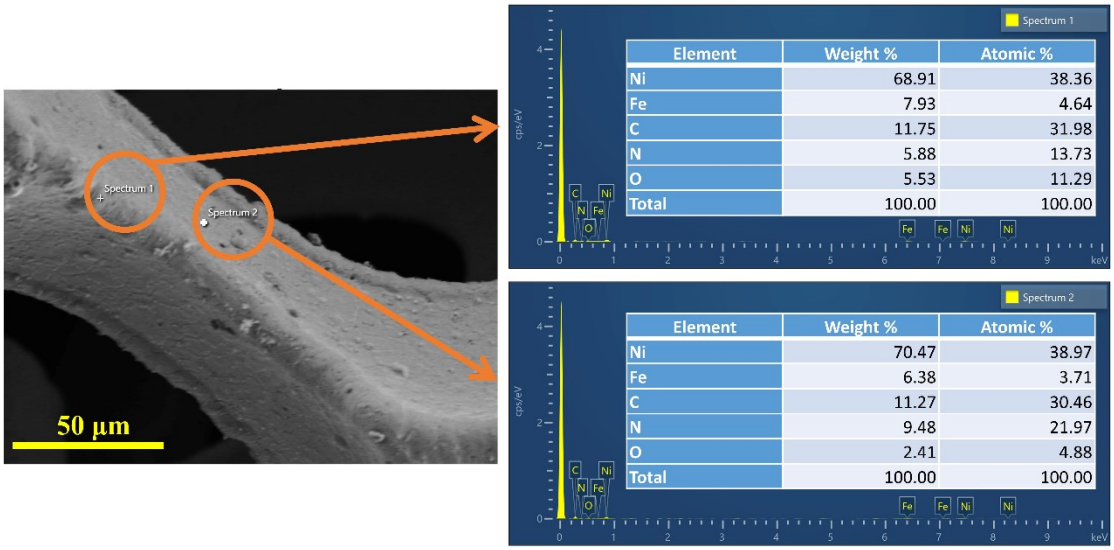

Fig. S2 SEM-EDX spectra of NiFe-PBA-NF.

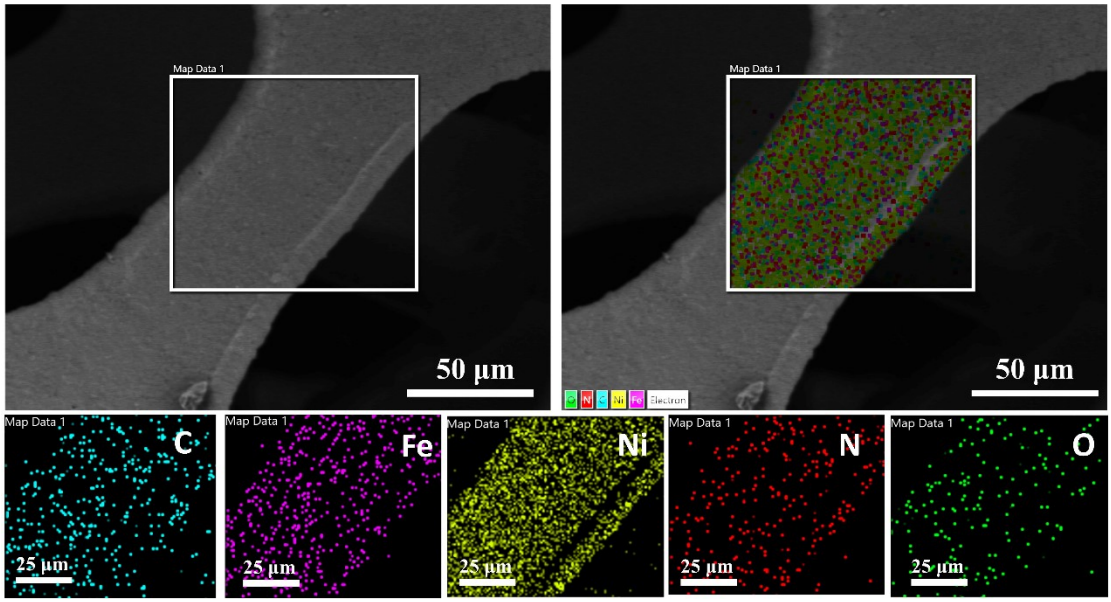

Fig. S3 SEM-EDX elemental mapping images of NiFe-PBA-NF.

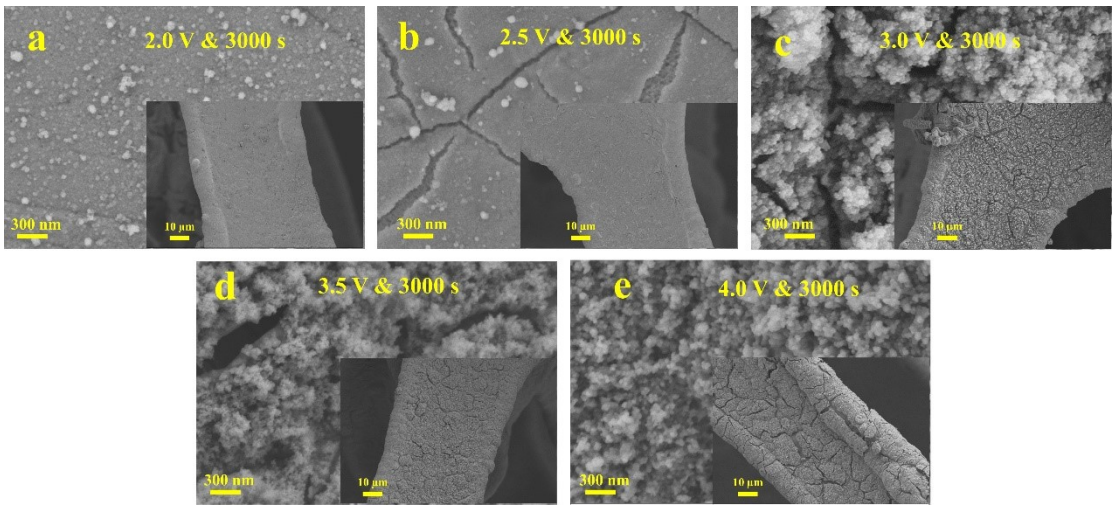

Fig. S4 SEM images of the NiFe-PBA-NF electrodes fabricated at different applied potentials with 3000 s.

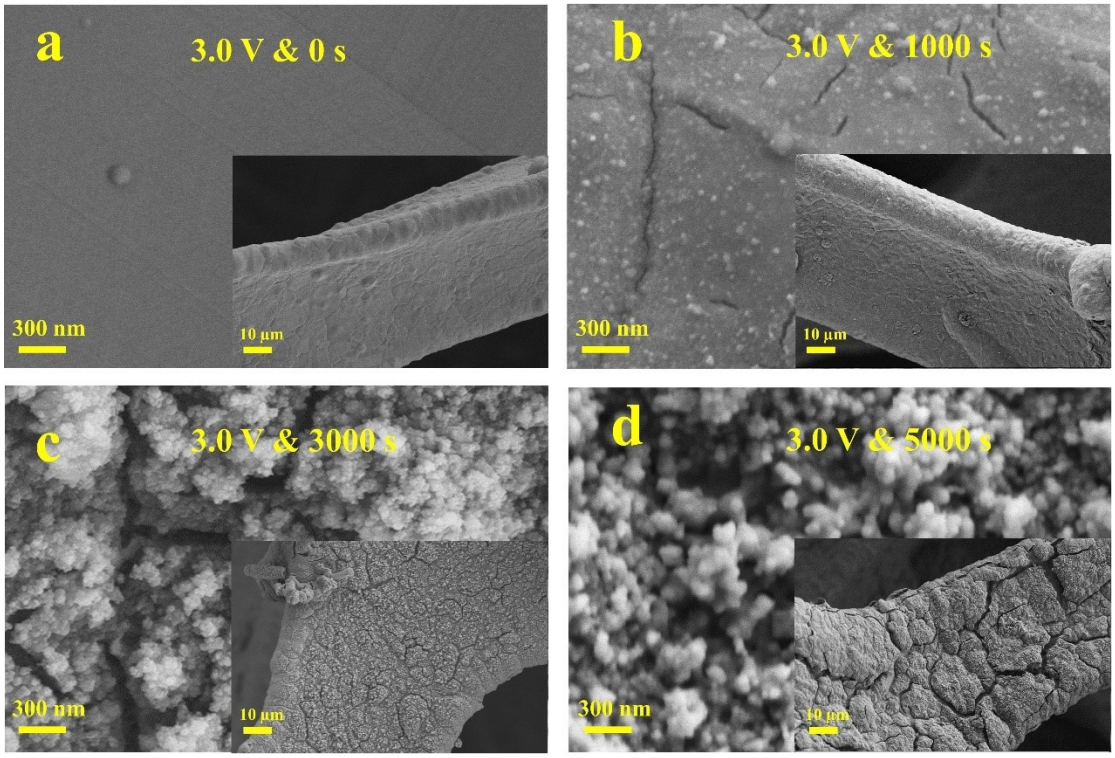

Fig. S5 SEM images of the NiFe-PBA-NF electrodes fabricated at 3.0 V with different reaction time.

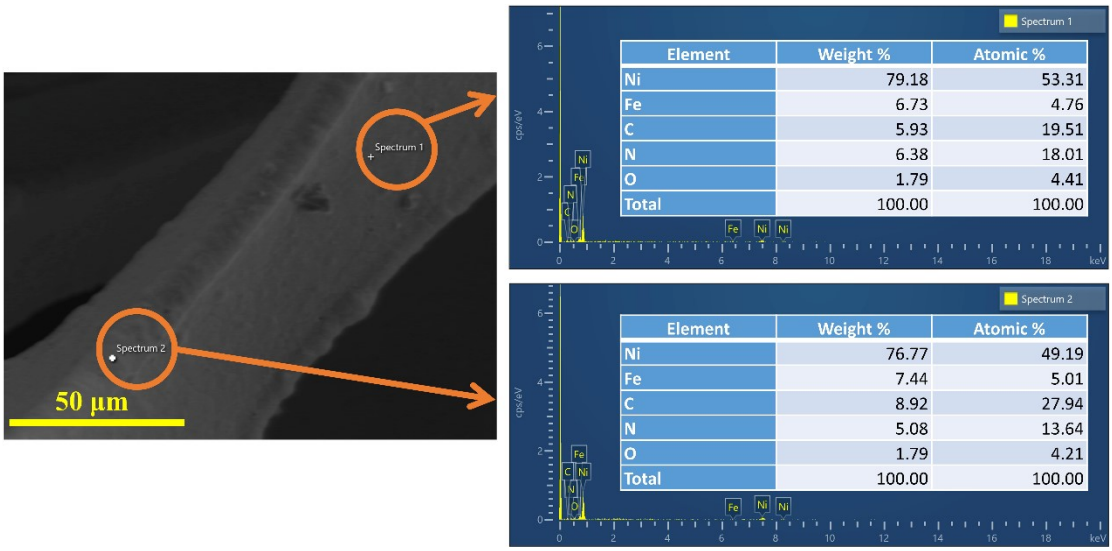

Fig. S6 SEM-EDX spectra of the NiFe-PBA-NF electrode fabricated at 2.5 V with reaction time of 3000 s.

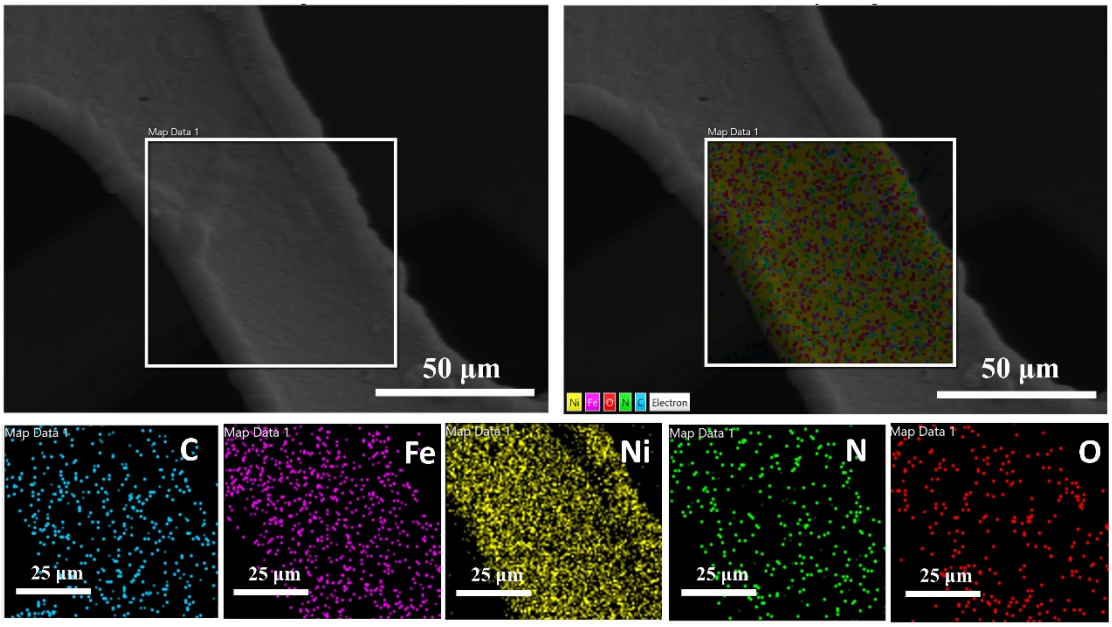

Fig. S7 SEM-EDX elemental mapping images of the NiFe-PBA-NF electrode fabricated at 2.5 V with reaction time of 3000 s.

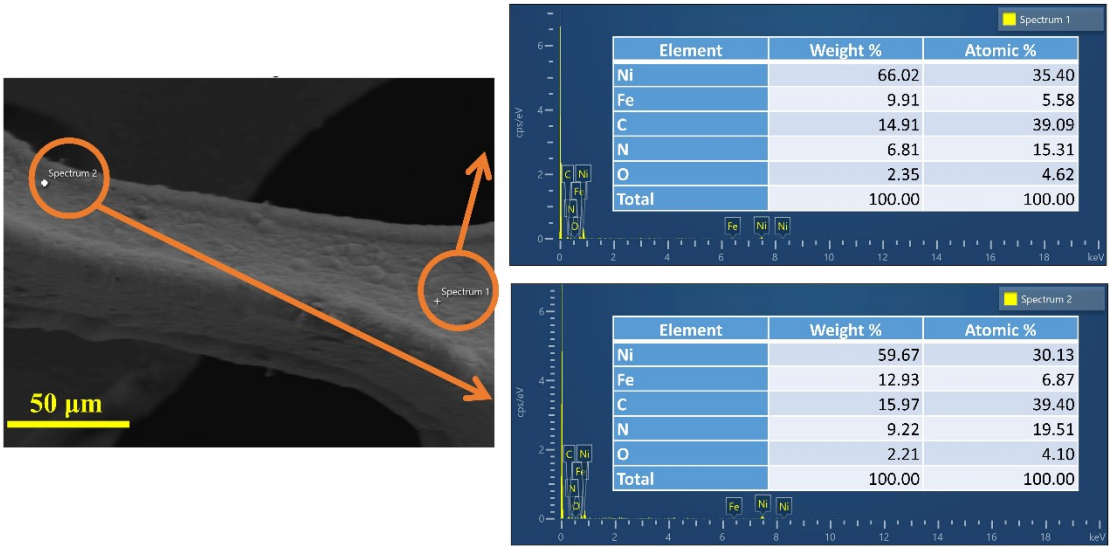

Fig. S8 SEM-EDX spectra of the NiFe-PBA-NF electrode fabricated at 3.5 V with reaction time of 3000 s.

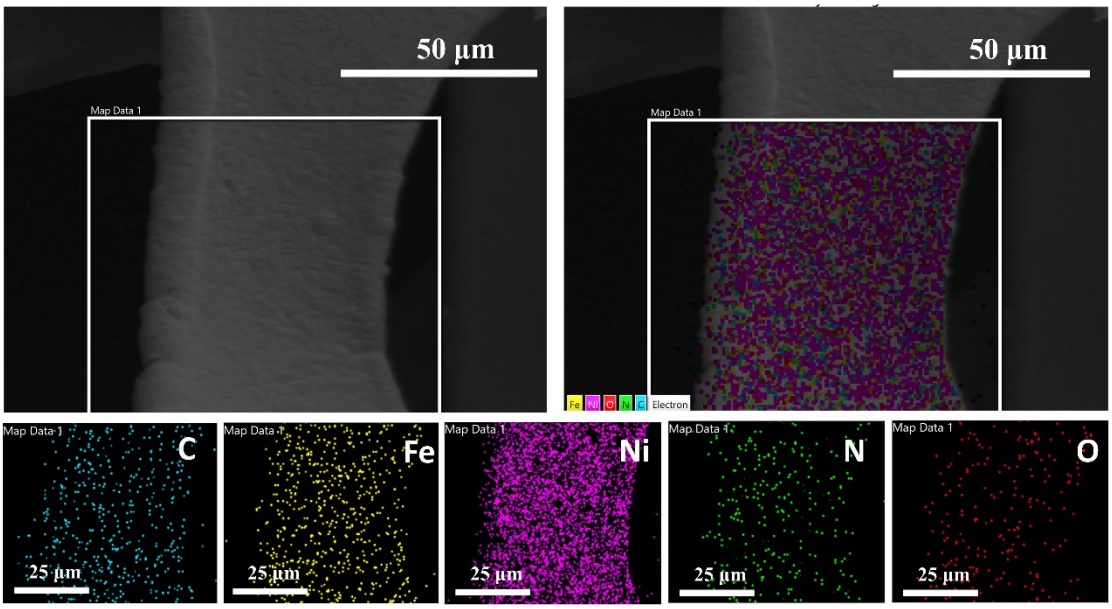

Fig. S9 SEM-EDX elemental mapping images of the NiFe-PBA-NF electrode fabricated at 3.5 V with reaction time of 3000 s.

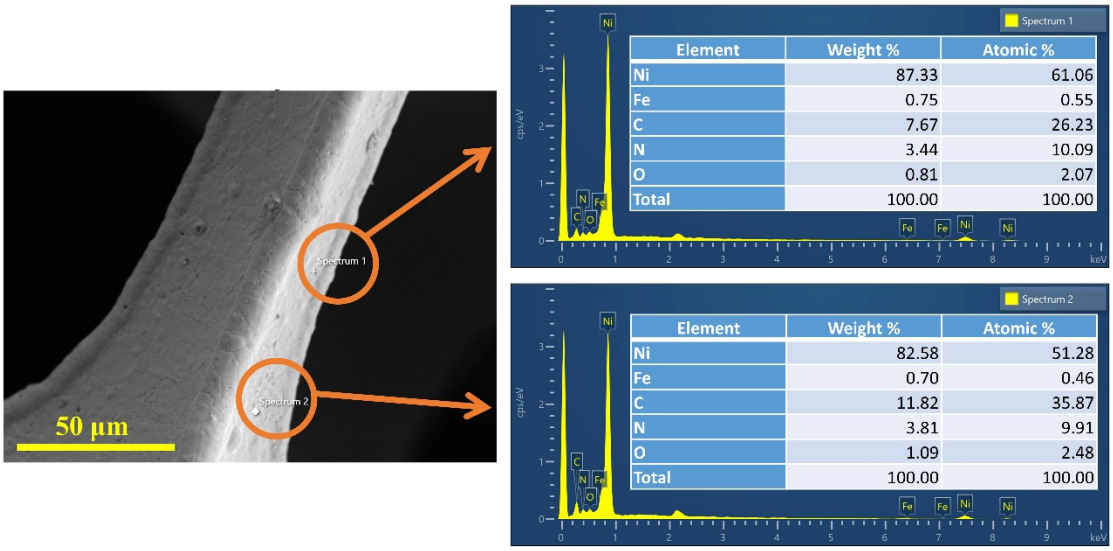

Fig. S10 SEM-EDX spectra of the NiFe-PBA-NF electrode fabricated at 3.0 V with reaction time of 1000 s.

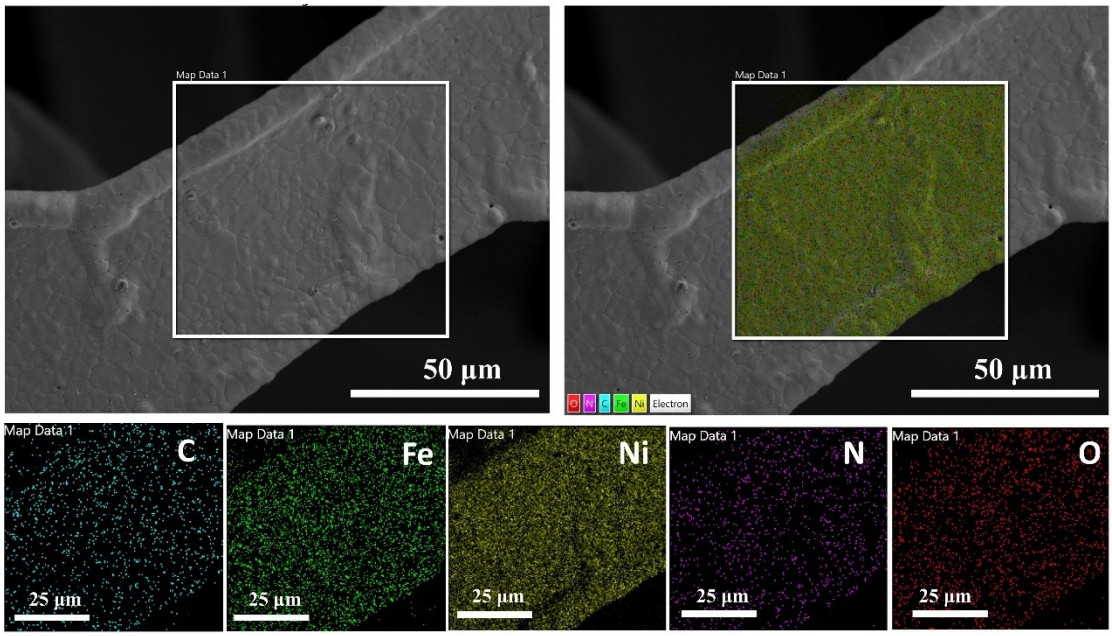

Fig. S11 SEM-EDX elemental mapping images of the NiFe-PBA-NF electrode fabricated at 3.0 V with reaction time of 1000 s.

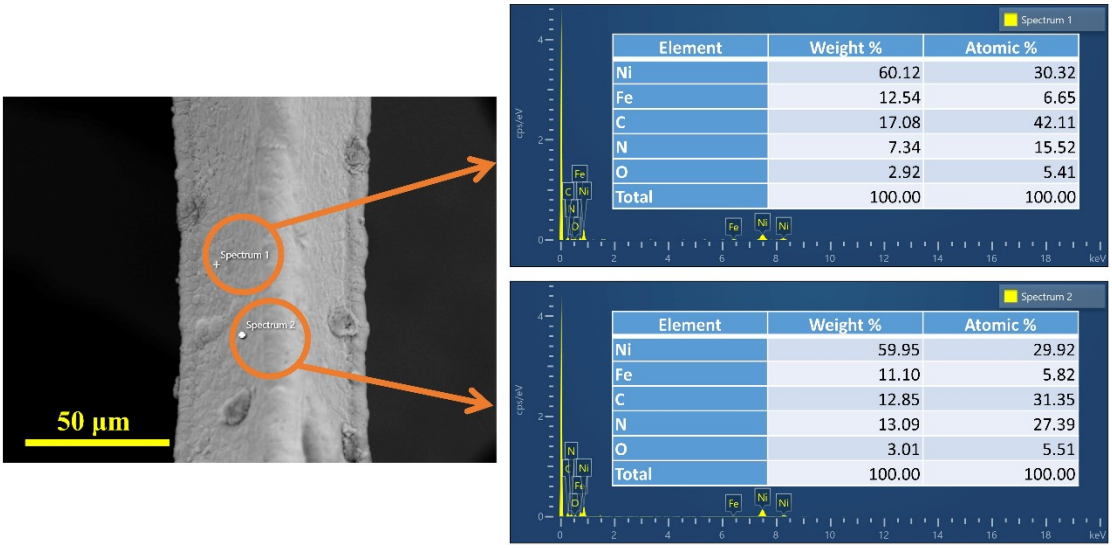

Fig. S12 SEM-EDX spectra of the NiFe-PBA-NF electrode fabricated at 3.0 V with reaction time of 5000 s.

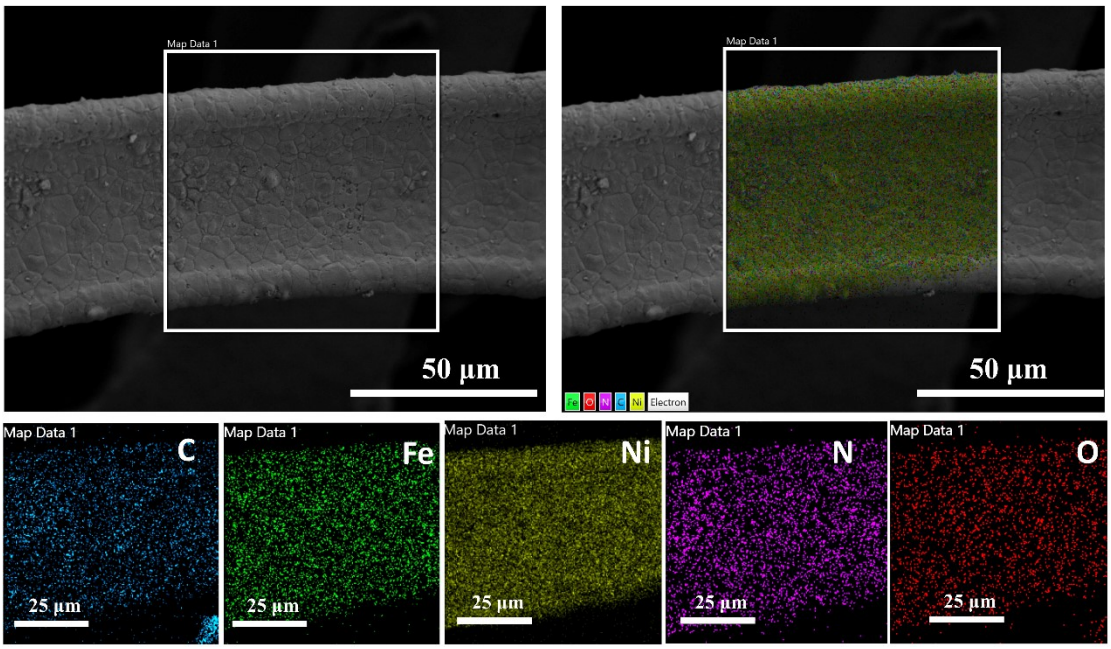

Fig. S13 SEM-EDX elemental mapping images of the NiFe-PBA-NF electrode fabricated at 3.0 V with reaction time of 5000 s.

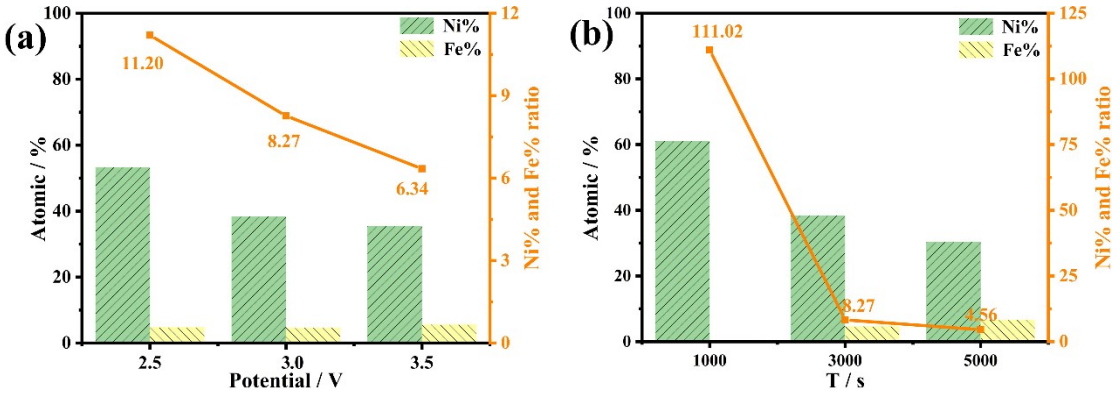

Fig. S14 The Ni/Fe ratios of the NiFe-PBA-NF electrodes fabricated at (a) different applied potentials, and (b) different reaction time at 3.0 V.

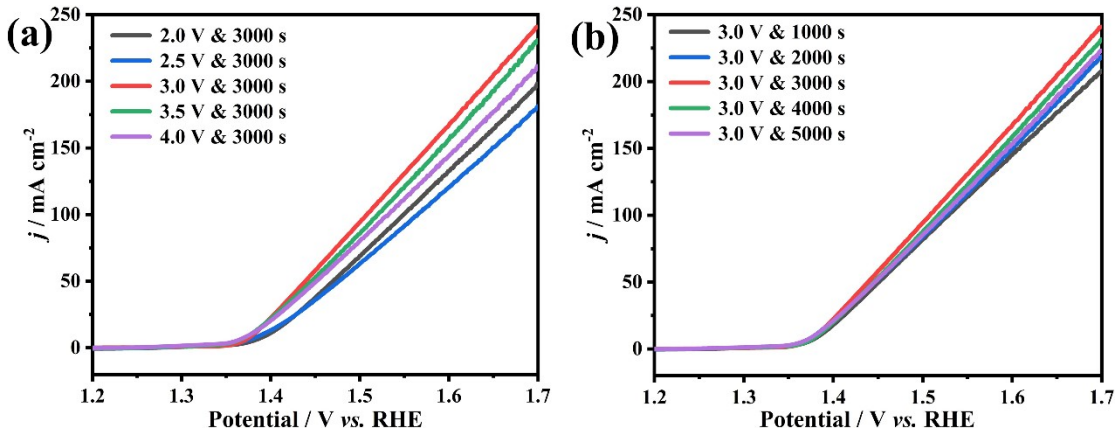

Fig. S15 UOR performance of the as-prepared NiFe-PBA-NF electrodes at (a) different applied potentials and (b) different reaction time at 3.0 V.

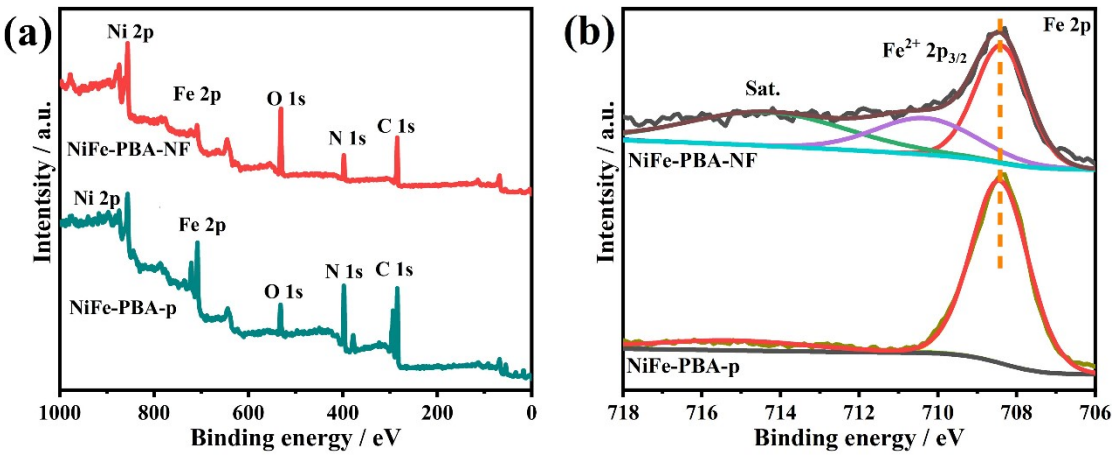

Fig. S16 (a) Survey and (b) Fe 2p XPS spectra of NiFe-PBA-NF and NiFe-PBA-p.

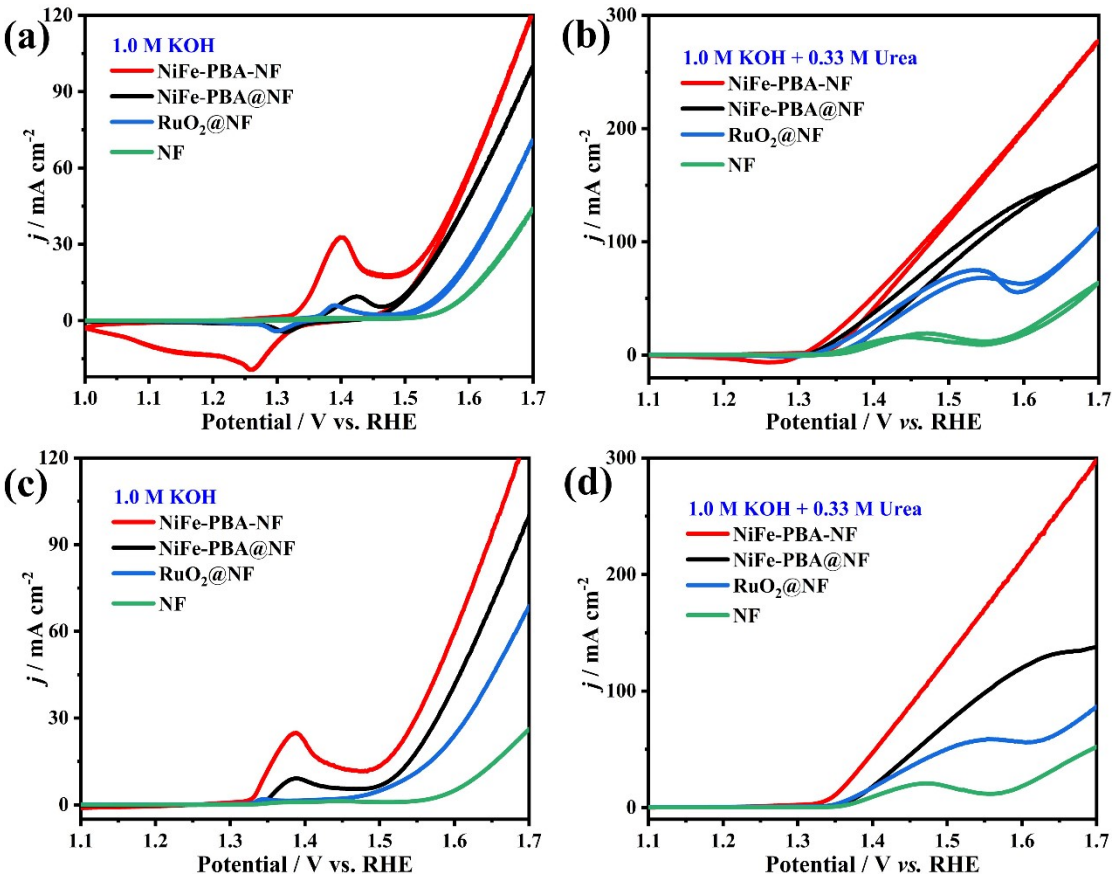

Fig. S17 (a, b) CV and (c, d) LSV curves of NiFe-PBA-NF, NiFe-PBA@NF, RuO_2@NF and NF in 1.0 M KOH with or without 0.33 M urea.

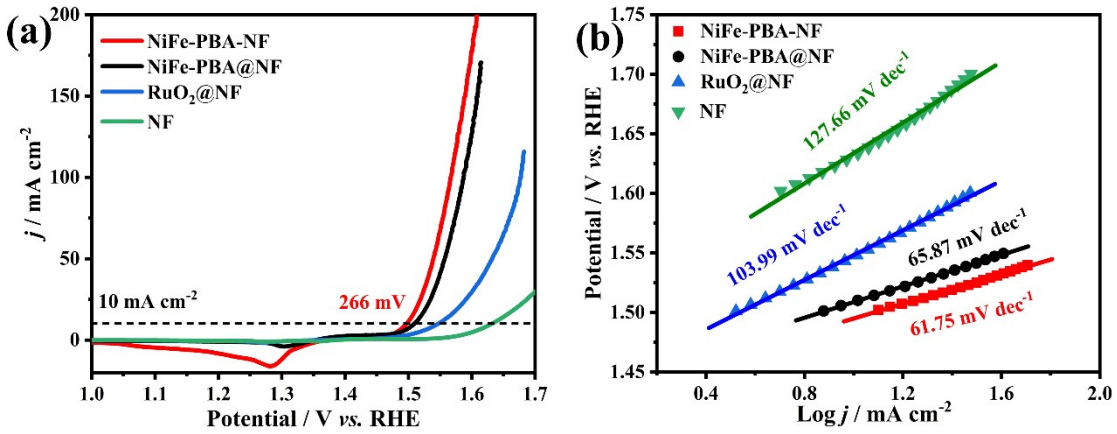

Fig. S18 (a) LSV curves of the as-prepared electrodes in the reverse sweep direction and (b) the corresponding Tafel plots in 1.0 M KOH.

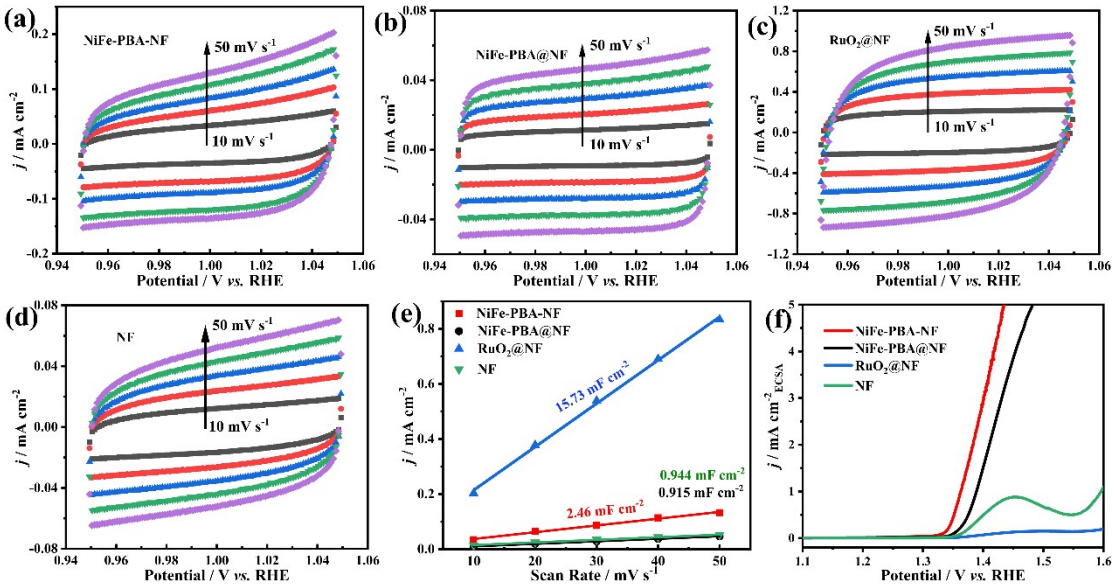

Fig. S19 ECSA measurements for NiFe-PBA-NF, NiFe-PBA@NF, RuO_2@NF and NF in 1.0 M KOH with 0.33 M urea. (a-d) CV curves at different scan rates. (e) Capacitance Δj ($= j_a - j_c$) against scan rates. (f) LSV curves normalized by ECSAs.

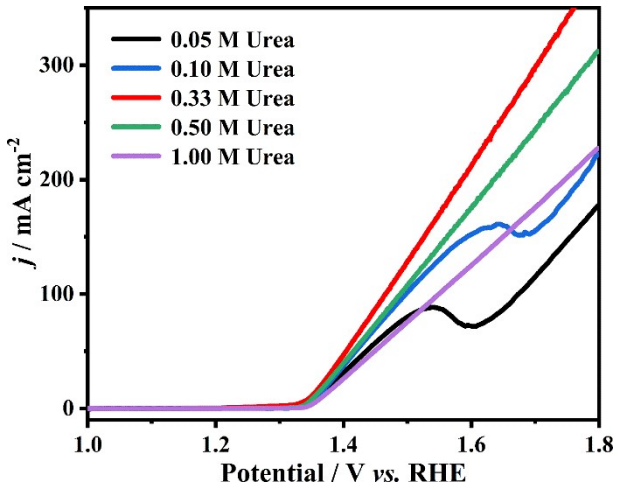

Fig. S20 LSV curves of NiFe-PBA-NF collected in 1.0 M KOH with different concentrations of urea.

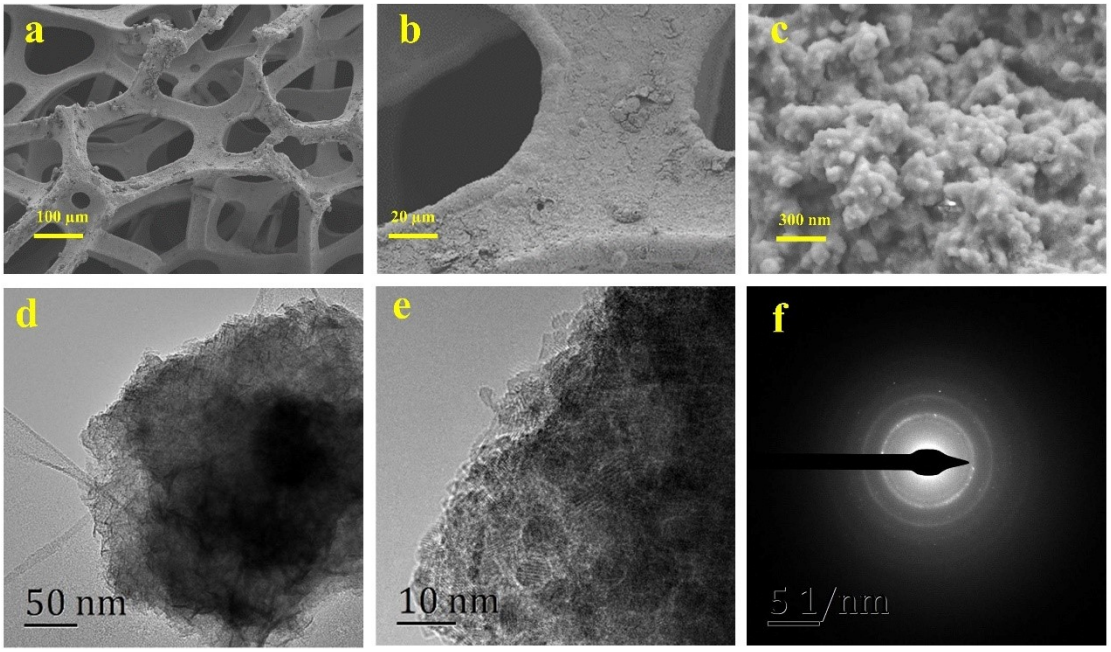

Fig. S21 (a-c) SEM and (d, e) TEM images, and (f) selected area electron diffraction pattern (SAED) pattern of NiFe-PBA-NF after UOR measurement.

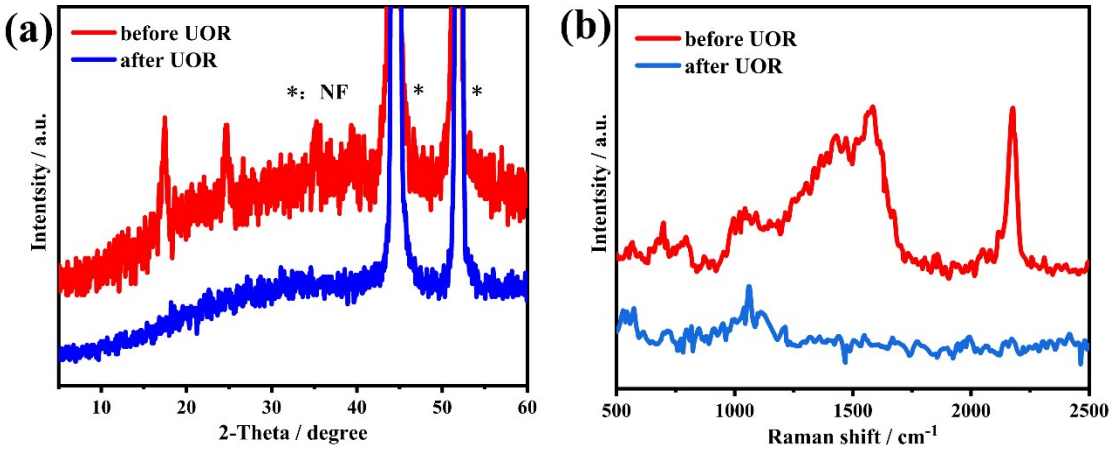

Fig. S22 (a) PXRD patterns and (b)Raman spectra of NiFe-PBA-NF before and after UOR measurement.

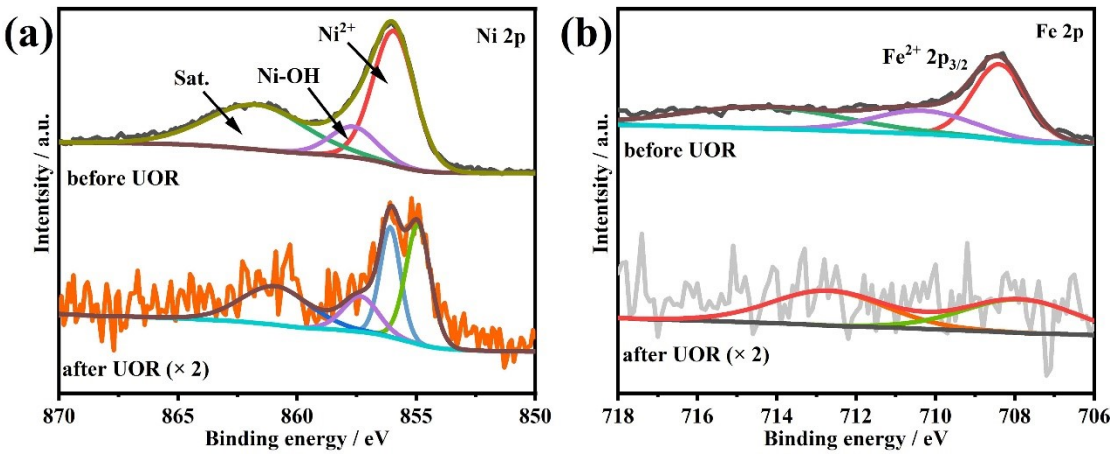

Fig. S23 (a) Ni 2p and (b) Fe 2p spectra of NiFe-PBA-NF before and after UOR measurement.

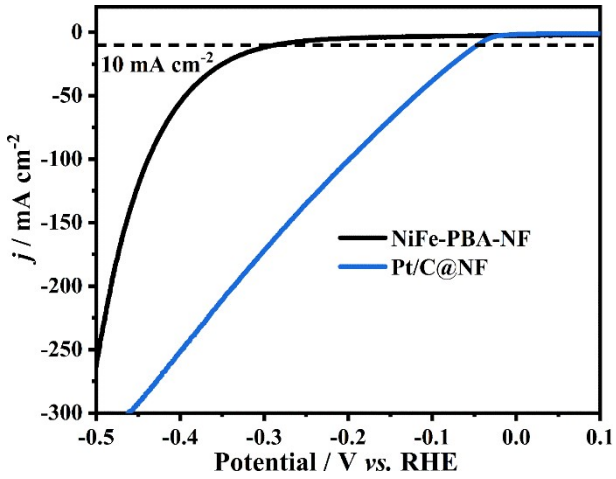

Fig. S24 LSV curves of NiFe-PBA-NF and Pt/C@NF in 1.0 M KOH with 0.33 M urea.

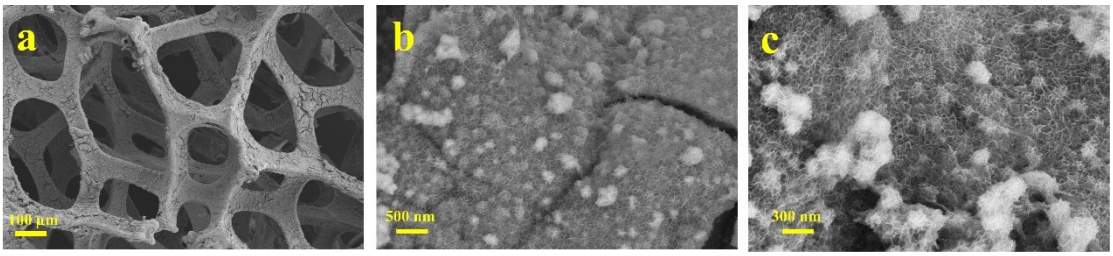

Fig. S25 SEM images of Ru-NiFe-PBA-NF.

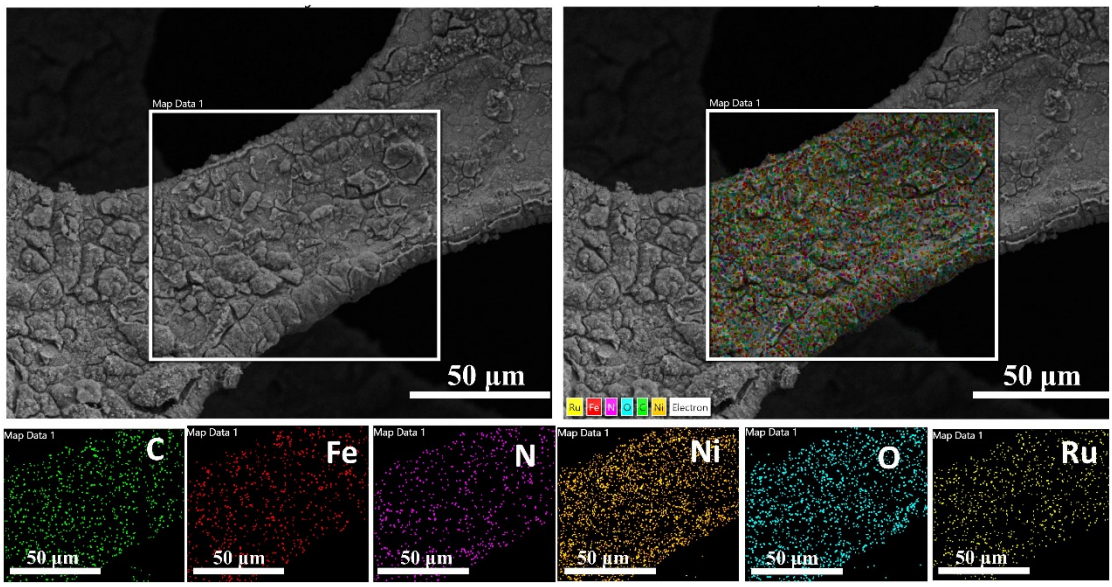

Fig. S26 SEM-EDX elemental mapping images of Ru-NiFe-PBA-NF.

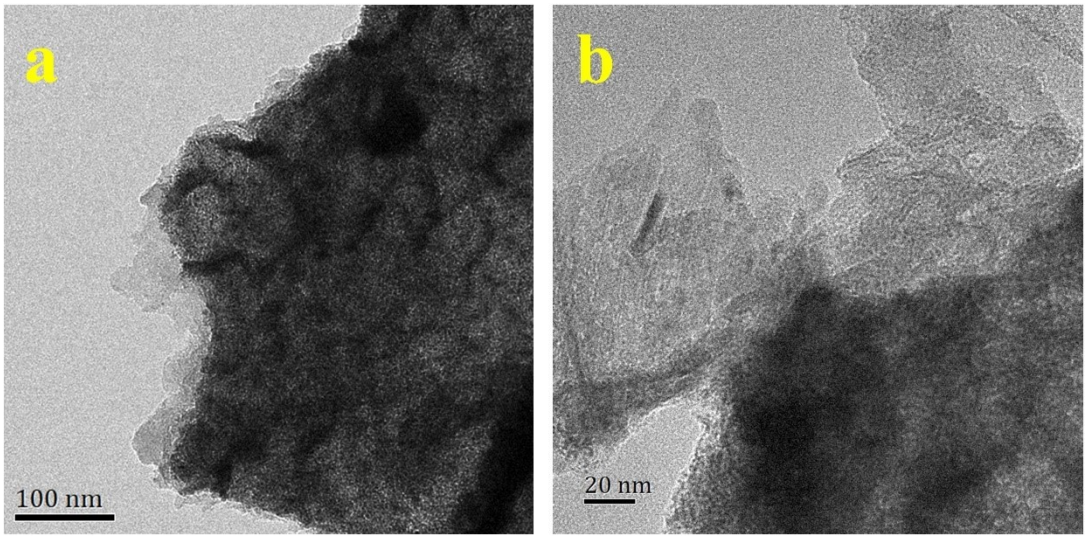

Fig. S27 TEM and HRTEM images of Ru-NiFe-PBA-NF.

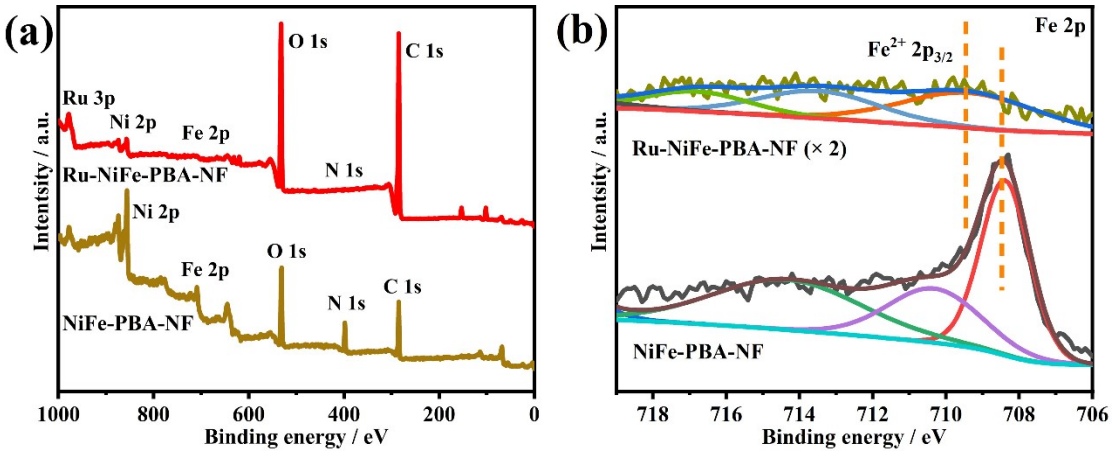

Fig. S28 (a) Survey and (b) Fe 2p XPS spectra of Ru-NiFe-PBA-NF and NiFe-PBA-NF.

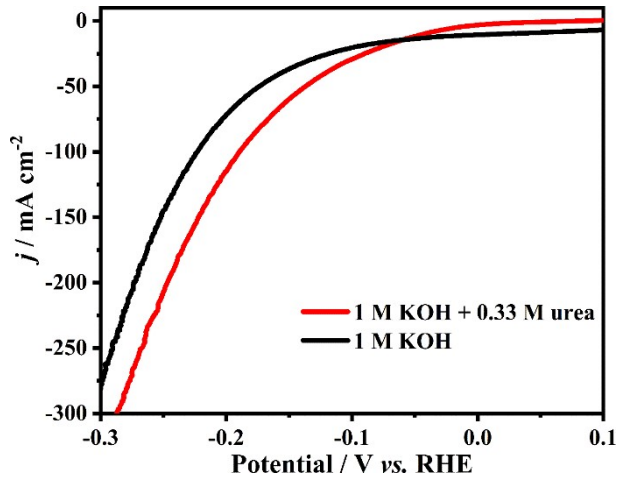

Fig. S29 LSV curves of Ru-NiFe-PBA-NF in 1.0 M KOH with and without 0.33 M urea.

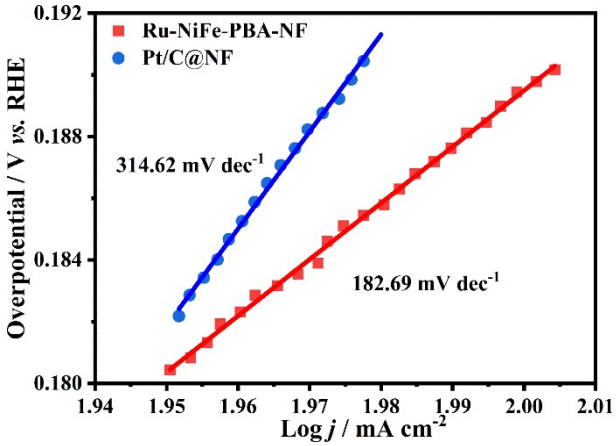

Fig. S30 Tafel plots of Ru-NiFe-PBA-NF and Pt/C@NF at the overpotential region larger than 0.18 V.

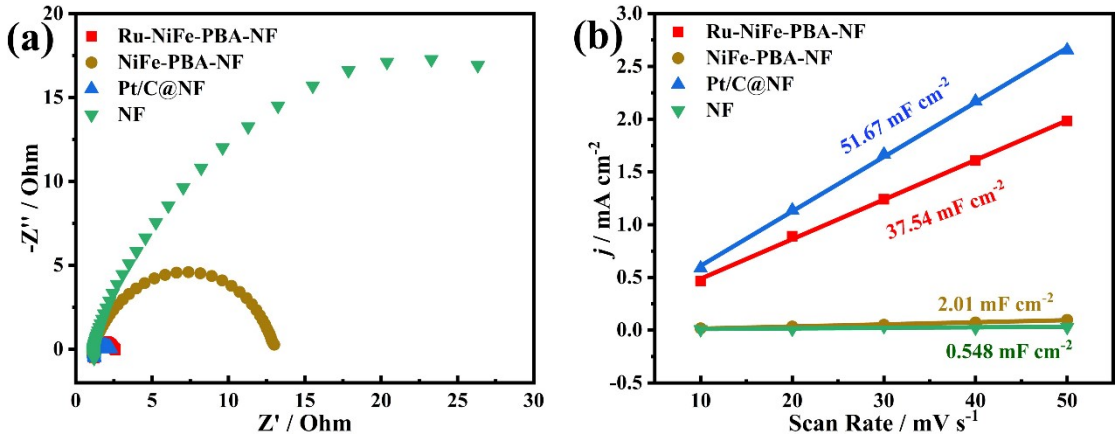

Fig. S31 (a) EIS plots and (b) capacitance Δj ($= j_a - j_c$) against scan rates of Ru-NiFe-PBA-NF, NiFe-PBA-NF, Pt/C@NF and NF in 1.0 M KOH with 0.33 M urea.

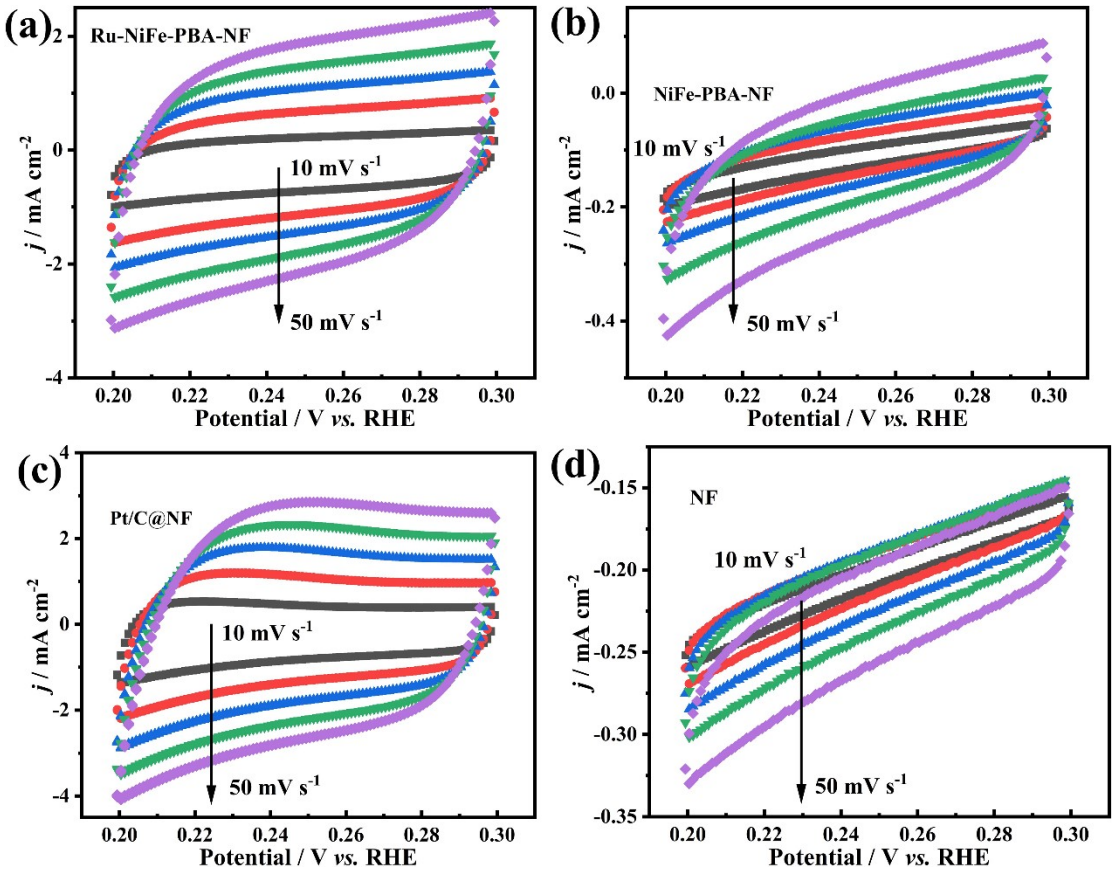

Fig. S32 (a-d) CV curves at different scan rates for Ru-NiFe-PBA-NF, NiFe-PBA-NF, Pt/C@NF and NF in 1.0 M KOH with 0.33 M urea.

Table S1 Comparison of the UOR performance of the recently reported Ni-based and other transition metal-based electrocatalysts**.**

Electrocatalysts	Electrolyte	Potentials@j_{UOR} (V @ mA cm^{-2})	Tafel slope (mV dec^{-1})	Refs.
NiFe-PBA-NF	**1.0 M KOH + 0.33 M urea**	**1.339 @ 10 1.375 @ 100**	**30**	**This work**
pa-NiFe LDH NS/NIF	1.0 M KOH + 0.33 M urea	1.459 @ 100	33	1
NiFeRh-LDH	1.0 M KOH + 0.33 M urea	1.346 @ 10	35	2
NiMoV LDH/NF	1.0 M KOH + 0.33 M urea	1.4 @ 100	24	3
CoFeCr LDH/NF	1.0 M KOH + 0.33 M urea	1.41 @ 100	85	4
$Ni(OH)_2$@NF	1.0 M KOH + 0.33 M urea	1.44 @ 100	24	5
NiClO-D	1.0 M KOH + 0.33 M urea	1.44 @ 100	41	6
NFO powders	1.0 M KOH + 0.33 M urea	1.4 @ 100	26	7
$CuCo_2O_4$	1.0 M KOH + 0.33 M urea	1.44 @ 100	46	8
1%Cu: $Ni(OH)_2$/NF	1.0 M KOH + 0.33 M urea	1.41@ 100	42	9
N-NiS/NiS_2	1.0 M KOH + 0.33 M urea	1.47 @ 100	28	10
porous $Ni(OH)_2$ nanosheet	1.0 M KOH + 0.33 M urea	1.59 @ 100	43	11
FeNi-MOF NSs	1.0 M KOH + 0.33 M urea	1.361 @ 10 1.385 @ 100	28	12
NP-NiFe (NP-$Ni_{0.7}Fe_{0.3}$)	1.0 M KOH + 0.33 M urea	1.5 @ 100	38	13
Ni/NiO@NC	1.0 M KOH + 0.33 M urea	1.4@ 100	19	14
1%Fe: α-$Ni(OH)_2$/NF	1.0 M KOH + 0.33 M urea	1.4@ 100	35	15
$Ni(OH)_2$ nanoflakes	1.0 M KOH + 0.33 M urea	1.48@ 100	36	16

$NiFe(OH)_X$ nanoparticles/Ni foam	1.0 M KOH + 0.33 M urea	1.395@ 100	29	[17]
O-NiMoP/NF	1.0 M KOH + 0.5 M urea	1.41 @ 100	34	[18]
NF/NiMoO-Ar	1.0 M KOH + 0.5 M urea	1.37 @ 10 1.42 @ 100	19	[19]
MnO_2/NF	1.0 M KOH + 0.5 M urea	1.33 @ 10 1.45 @ 100	75	[20]
P-$CoNi_2S_4$	1.0 M KOH + 0.5 M urea	1.367 @ 100	55	[21]
NiCoP/CC	1.0 M KOH + 0.5 M urea	1.30 @ 10	49	[22]
CoS_2-MoS_2	1.0 M KOH + 0.5 M urea	1.29 @ 10	32	[23]
CoMn/$CoMn_2O_4$	1.0 M KOH + 0.5 M urea	1.32 @ 10 1.36 @ 100	38	[24]

Table S2 Comparison of the hybrid water electrolysis performance of the recently reported Ni-based and other transition metal-based electrocatalysts**.**

Catalyst	Organic compounds	electrolyte	Current density (mA cm^{-2})	Voltage (V)	Refs.
NiFe-PBA-NF//Ru-NiFe-PBA-NF	**0.33 M Urea**	**1 M KOH**	**10**	**1.36**	**This Work**
			50	**1.70**	
N-NiS/NiS_2	0.33 M Urea	1 M KOH	10	1.62	10
			50	~1.84	
FeNi-MOF NSs	0.33 M Urea	1 M KOH	10	1.43	12
			50	1.70	
NFO	0.33 M Urea	1 M KOH	10	1.455	15
			50	1.59	
Ni_2P/Ni-MOF@NF	0.33 M Urea	1 M KOH	10	1.50	25
PBA@MOF-Ni/Se	0.5 M Urea	1 M KOH	10	1.50	26
NF/NiMoO-Ar//NF/NiMoO-H_2	0.5 M Urea	1 M KOH	10	1.38	20
			50	1.48	
MOF-Ni@MOF-Fe-S	0.5 M Urea	1 M KOH	10	1.539	27
			50	~1.75	
CoS_x/Co-MOF	0.5 M Urea	1 M KOH	10	1.48	28
			50	~1.70	
Ni-MOF-0.5/NF	0.5 M Urea	1 M KOH	10	1.52	29

			50	~1.71	
Ni-Mo nanotube	0.1 M Urea	1 M KOH	10	1.43	[30]
			50	~1.64	
F modified β-FeOOH	10 mM Ethanol	1 M KOH	10	1.43	[31]
Ni_3S_2/NF	10 mM HMF	1 M KOH	10	1.46	[32]
			50	1.58	
Ni_2P/NF	10 mM HMF	1 M KOH	10	1.44	[33]
			50	1.58	
Ni_2P/Ni/NF	30 mM Furfural	1 M KOH	10	1.48	[34]
3D hierarchically porous nickel	10 mM Benzyl alcohol	1 M KOH	10	1.50	[35]
			50	1.60	

References:

1. J. Xie, H. Qu, F. Lei, X. Peng, W. Liu, L. Gao, P. Hao, G. Cui and B. Tang, *J. Mater. Chem. A*, 2018, **6**, 16121–16129.

2. H. Sun, W. Zhang, J.-G. Li, Z. Li, X. Ao, K.-H. Xue, K. K. Ostrikov, J. Tang and C. Wang, *Appl. Catal. B: Environ.*, 2021, **284**, 119740.

3. Z. Wang, W. Liu, J. Bao, Y. Song, X. She, Y. Hua, G. Lv, J. Yuan, H. Li and H. Xu, *Chem. Eng. J.*, 2022, **430**, 133100.

4. Z. Wang, W. Liu, Y. Hu, M. Guan, L. Xu, H. Li, J. Bao and H. Li, Appl. Catal. B: Environ., 2020, **272**,118959.

5. L. Xia, Y. Liao, Y. Qing, H. Xu, Z. Gao, W. Li and Y. Wu, *ACS Appl. Energy Mater.*, 2020, **3**, 2996–3004.

6. L. Zhang, L. Wang, H. Lin, Y. Liu, J. Ye, Y. Wen, A. Chen, L. Wang, F. Ni, Z. Zhou, S. Sun, Y. Li, B. Zhang and H. Peng, *Angew. Chem., Int. Ed.*, 2019, **131**, 16976–16981.

7. F. Wu, G. Ou, J. Yang, H. Li, Y. Gao, F. Chen, Y. Wang and Y. Shi, *Chem. Commun.*, 2019, **55**, 6555–6558.

8. C. Zequine, F. Wang, X. Li, D. Guragain, S. R. Mishra, K. Siam, P. Kahol and R. Gupta, *Appl. Sci.*, 2019, **9**, 793.

9. J. Xie, L. Gao, S. Cao, W. Liu, F. Lei, P. Hao, X. Xia and B. Tang, *J. Mater. Chem. A*, 2019, **7**, 13577–13584.

10. H. Liu, Z. Liu, F. Wang and L. Feng, *Chem. Eng. J.*, 2020, **397**, 125507.

11. W. Yang, X. Yang, B. Li, J. Lin, H. Gao, C. Hou and X. Luo, *J. Mater. Chem. A*,

2019, **7**, 26364–26370.

12. X. Zhang, X. Fang, K. Zhu, W. Yuan, T. Jiang, H. Xue and J. Tian, *J. Power Sources*, 2022, **520**, 230882.

13. Z. Cao, T. Zhou, X. Ma, Y. Shen, Q. Deng, W. Zhang and Y. Zhao, *ACS Sustainable Chem. Eng.*, 2020, **8**, 11007–11015.

14. X. Ji, Y. Zhang, Z. Ma and Y. Qiu, *ChemSusChem*, 2020, **13**, 5004–5014.

15. J. Xie, W. Liu, F. Lei, X. Zhang, H. Qu, L. Gao, P. Hao, B. Tang and Y. Xie, *Chem. Eur. J.*, 2018, **24**, 18408–18412.

16. W. Yang, X. Yang, C. Hou, B. Li, H. Gao, J. Lin and X. Luo, *Appl. Catal. B: Environ.*, 2019, **259**,118020.

17. X. L. Yang, Y. W. Lv, J. Hu, J. R. Zhao, G. Y. Xu, X. Q. Hao, P. Chen and M. Q. Yan, *RSC Adv*, 2021, **11**, 17352-17359.

18. H. Jiang, M. Sun, S. Wu, B. Huang, C. S. Lee and W. Zhang, *Adv. Funct. Mater.*, 2021, **31**, 2104951.

19. Z.-Y. Yu, C.-C. Lang, M.-R. Gao, Y. Chen, Q.-Q. Fu, Y. Duan and S.-H. Yu, *Energy Environ. Sci.*, 2018, **11**, 1890–1897.

20. S. Chen, J. Duan, A. Vasileff and S. Z. Qiao, *Angew. Chem., Int. Ed.*, 2016, **55**, 3804–3808.

21. X. F. Lu, S. L. Zhang, W. L. Sim, S. Gao and X. W. D. Lou, *Angew. Chem., Int. Ed.*, 2021, **133**, 23067–23073.

22. L. Sha, J. Yin, K. Ye, G. Wang, K. Zhu, K. Cheng, J. Yan, G. Wang and D. Cao, *J. Mater. Chem. A*, 2019, **7**, 9078–9085.

23. C. Li, Y. Liu, Z. Zhuo, H. Ju, D. Li, Y. Guo, X. Wu, H. Li and T. Zhai, *Adv. Energy Mater.*, 2018, **8**, 1801775.

24. C. Wang, H. Lu, Z. Mao, C. Yan, G. Shen and X. Wang, *Adv. Funct. Mater.*, 2020, **30**, 2000556.

25. H. Wang, H. Zou, Y. Liu, Z. Liu, W. Sun, K. A. Lin, T. Li and S. Luo, Scientific Reports, 2021, 11, **1**, 21414.

26. H. Xu, K. Ye, K. Zhu, Y. Gao, J. Yin, J. Yan, G. Wang and D. Cao, Inorganic Chemistry Frontiers, 2021, **8**, 2788–2797.

27. H. Xu, K. Ye, K. Zhu, J. Yin, J. Yan, G. Wang and D. Cao, *Dalton Trans.*, 2020, **49**, 5646–5652.

28. H. Xu, K. Ye, K. Zhu, J. Yin, J. Yan, G. Wang and D. Cao, *Inorg. Chem. Front.*, 2020, **7**, 2602–2610.

29. S. Zheng, Y. Zheng, H. Xue and H. Pang, *Chem. Eng. J.*, 2020, **395**, 125166.

30. J.-Y. Zhang, T. He, M. Wang, R. Qi, Y. Yan, Z. Dong, H. Liu, H. Wang and B. Y. Xia, *Nano Energy*, 2019, **60**, 894–902.

31. G.-F. Chen, Y. Luo, L.-X. Ding and H. Wang, *ACS Catal.*, 2018, **8**, 526–530.

32. B. You, X. Liu, N. Jiang and Y. Sun, *J. Am. Chem. Soc.*, 2016, **138**, 13639–13646.

33. B. You, N. Jiang, X. Liu and Y. Sun, *Angew. Chem., Int. Ed.*, 2016, **55**, 9913–9917.

34. N. Jiang, X. Liu, J. Dong, B. You, X. Liu and Y. Sun, *ChemNanoMat.*, 2017, **3**, 491–495.

35. B. You, X. Liu, X. Liu and Y. Sun, *ACS Catal.*, 2017, **7**, 4564–4570.